Defining absolute permeability for CO_2 injection projects: scope for increased economic storage capacity

Jos G. Maas[1*], *Dario* Santonico[1], *Albert* Hebing[1], and *Niels* Springer[2]

[1]PanTerra Geoconsultants B.V., Leiderdorp, The Netherlands
[2]GEUS, Copenhagen, Denmark

Abstract. Single phase brine permeability, also reported as "absolute brine permeability", is typically used as reference value in CO_2 drainage experiments to normalise relative permeability data. However, using the brine absolute permeability to normalise relative permeabilities creates an unexpected problem in the event that the (Klinkenberg-corrected) gas permeability is larger than the absolute brine permeability. To explain: late in the displacement of brine by a non-wetting phase, at low brine saturation, the effective gas permeability will necessarily approach the single phase gas permeability giving rise to gas relative permeabilities above unity when normalised to the absolute brine permeability. This indeed also has been observed in the laboratory. In itself, such relative permeability values are a viable result. However, commercial reservoir simulators do not allow relative permeabilities to be input with values above unity. In our experience, in line with data reported by many authors, the absolute gas permeability often is larger than the brine permeability. Low brine saturations particularly do occur close to the injector in the field. Therefore, the issue around relative permeabilities being above unity is very relevant estimating CO_2 well injectivity and therefore for simulating CCS field behaviour on the whole.

To determine whether lower absolute brine permeabilities are a laboratory artefact or representative of field conditions, we conducted flow experiments on ceramic plugs and clean lithology outcrop Obernkirchener (OBKN) sandstone samples and conducted a rigorous statistical analysis on the results. We found the brine absolute permeabilities reproducible and insensitive to brine composition and equilibration time of the plugs in brine. Ceramic plugs exhibited brine permeabilities equal to the gas permeabilities with high statistical probability. The OBKN samples had brine permeabilities with a factor of around 0.7 lower than the gas permeabilities. We attribute this behaviour to ionic forces active between the rock surface and the ions in the brine.

Subsequently, we adapted the SCAL simulator SCORES to accept relative permeabilities larger than 1 and found that the generated production, pressure drop and saturation profiles with input normalised to the brine permeability, duplicated the profiles generated with the relative permeabilities normalised to the gas permeability. This tallies with what one finds analysing the flow equations in terms of re-normalising relative permeabilities. Therefore, our recommendation is to use the Klinkenberg-corrected gas permeability as the absolute permeability to normalise CO_2-brine relative permeabilities. We show that this may well have a positive effect on the economic storage capacity.

1 Introduction

First we present a historic overview on how absolute permeability came into being; subsequently we discuss how "absolute" turned out to be less absolute than expected. Permeability of rock was originally defined by Henry Darcy in 1856 [1]. In many if not all textbooks on core analysis or reservoir engineering (see e.g. Scheidegger [2], Collins [3], Dake [4], Warner [5]), absolute permeability is defined to be a rock property, i.e. it is a property not depending on choice of fluid, flow rate, etc.. The practical application of that was investigated by Klinkenberg in 1941 [6], showing the equivalency of liquid (different oils and "water") and gas permeability (after applying the correction that he developed).

A common approach followed in Routine Core Analysis (RCA) and Special Core Analysis (SCAL) measurement programs is to measure the Klinkenberg-corrected[1] gas permeability as a base data point, but generally that number does not play a role in the subsequent laboratory

[1] In the remainder of the paper, we will use "gas permeability" to indicate "Klinkenberg-corrected gas permeability".

* Corresponding author: jgmaas@gmail.com

work, except possibly in Digital Rock Physics (DRP, see [7]) or for rock typing and/or for building correlations [8, 9]. Conventionally, the next step in the measurement program is to saturate the core plug with brine of some prescribed composition and to measure the single-phase "absolute brine permeability". In line with our own experience, often the single-phase brine permeability K_{brine} is significantly lower than the gas permeability K_{gas}. A reduction by ⅓ to ½ is not unusual, and sometimes even stronger reductions are seen to a factor of 10 or so (see Orlander [8], Saidi [9], Tanikawa [10], Ahmad [11], Zaidin [12]). Contrary to K_{gas} data, K_{brine} data play an important role in reservoir engineering. K_{brine} may be used e.g. as a screening parameter for field development. In addition, K_{brine} may be used as a reference value in the calculation of relative permeabilities, although in the industry other reference values are used as well (see e.g. Cable and Burke [13]), such as the effective permeability to oil at initial water saturation (S_{wi}). The choice of reference value is determined by each service provider in consultation with the operating company.

It is recognised by several authors (McPhee and Arthur [14], Mikkelsen and Scheie [15], Cable et al. [16]) that the effective oil permeability at S_{wi} can be found to be larger than K_{brine}, giving rise to relative permeability values beyond unity. This is then explained as the "lubrication effect" (see also [17, 18, 19, 20]) that is believed to occur due to the presence of brine filling smaller pores/pore throats thereby reducing the surface roughness of the pores, providing lubrication to the oil phase.

In addition, a complicating factor in measuring gas permeability is that turbulence reduces the gas permeability. This problem is well-known in the industry and can be managed by adhering to the API-RP40 guidelines [21]. Occasionally authors do not provide information on whether they followed these guidelines, which inhibits a good comparison with other literature data.

The RP40 document, although presently not actively supported by API anymore, shows a wealth of well-documented plots that are very useful avoiding e.g. turbulence or other distorting effects on permeability measurements. We have made use of RP40 extensively in designing our experiments, see further Section 2.

For the current work, we have focused on the observation that the effective oil permeability may be larger than K_{brine}, but smaller or maximally equal to K_{gas}. Rather than bringing in a possible lubrication effect to explain higher effective oil permeability, we suggest to accept that K_{brine} is lower than K_{gas} due to interaction of the brine with the rock. At the same time, we aimed to establish whether the reduced K_{brine} was a laboratory artefact, or rather it is representative for the reservoir.

We considered two scenarios: clay interaction and ionic forces active between the rock surface and the ions in the brine. We have addressed this by designing experiments to measure the absolute (i.e. single-phase) permeability using different fluids and two rock types: ceramic plugs and outcrop Obernkirchener (OBKN) sandstone. Ceramic plugs were chosen to have samples that would be "inert" and have no electro-chemical interactions with brine. OBKN sandstone was chosen because it has a typical "clean" lithology, but not prone to clay swelling. The experimental work showed that it is plausible that the reduced K_{brine} is not a laboratory artefact and is presented in Section 2. In Section 3, we discuss the implications of relative permeabilities going above unity both for laboratory protocols as well as for reservoir simulations. In Section 4, we show how our findings may impact on the economics as part of CCS project screening. Results and Recommendations are summarised in Section 5.

2 Laboratory experiments

Discrepancies between gas and brine permeability measurements are commonly observed in core analysis and may arise from a range of factors, including fluid-rock interactions. Laboratory work was conducted at PanTerra Geoconsultants facilities to investigate relations between gas permeability, oil permeability and brine permeability under different salinities and conditions. Brine compositions are typically designed to be representative of reservoir formation water while minimizing the risk of clay swelling or fines mobilization, which can artificially reduce measured permeability.

2.1 Initial procedures

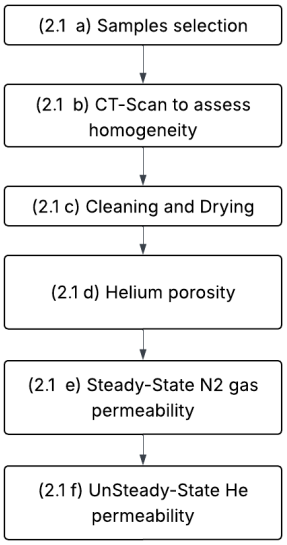

Fig. 1. Flow chart listing the initial experimental steps of the measurement program.

To differentiate between electro-chemical effects and physical flow mechanisms, four 1-inch diameter ceramic plug samples were tested. These ceramic samples provide a controlled porous medium with no expected fluid–solid interactions, serving as a baseline to identify purely physical effects. We conducted XRD on one ceramic sample at the end of the measurement program and it showed 100% Corundum (Al_2O_3).

In addition, four 1-inch diameter OBKN sandstone samples were selected. These are clean, well-sorted sandstones with minimal clay content [22] and can be considered being largely insensitive to clay interaction. This allows for controlled testing using a wide range of brine salinities. We verified clay content of the OBKN plugs at the end of the experimental program with XRD on one sample. It showed 94% quartz, 5% kaolinite, 1% albite and only traces (< 0.5%) of halite. This is in line with seen in the literature [22].

The experimental program consisted of many steps with QC steps at strategic points. The first part of the program is shown in Fig. 1.

To verify sample homogeneity, all plugs were scanned using helical 3D X-ray computed tomography (XCT), and V numbers were calculated following the methodology described in [23]. All samples exhibited V values around 0.1 or lower, indicating excellent homogeneity and suitability for the study. An example of a 3D XCT-Scan is shown in Fig. 2 and the V values are listed in Table 1.

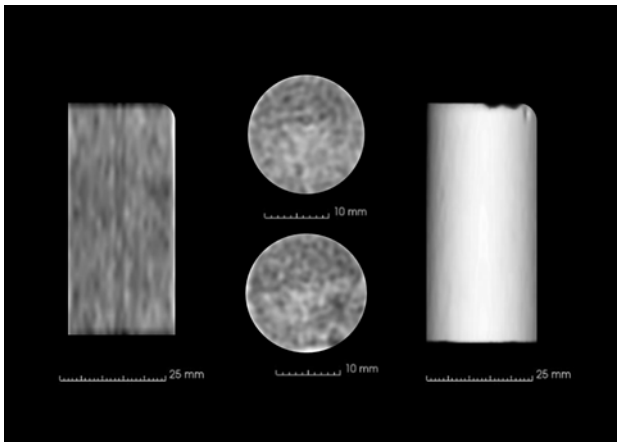

Fig. 2. Typical images collected by XCT of a core plug. In the centre two cross-sections are shown out of a series of many, taken in one sweep of a helical scan. The resolution is about 0.2 mm/pixel, slice thickness is 2 mm. The image to the left is a longitudinal reconstruction through a plane of choice using the data of all cross-sectional images together. The image to the right is a reconstruction along the outer surface.

Table 1. Homogeneity number V for each plug, calculated from the XCT cross-sectional data [23]. V = 0 indicates perfect homogeneity. Cut-off for normally distributed porosity plugs is 0.9 [23], so all plugs have excellent homogeneity.

Sample	V
C1	0.1
C2	0.14
C3	0.06
C4	0.06
OBKN1	0.1
OBKN2	0.1
OBKN3	0.1
OBKN4	0.1

All eight samples were subjected to a thorough cleaning process using a Soxhlet extraction setup with an azeotropic mixture of chloroform, methanol and water. The extraction was carried out continuously for a duration of 48 hours. Following the cleaning, samples were oven-dried at 95 °C until stable weight.

Subsequent to cleaning and drying, ambient helium pore volume and porosity were measured with our DAPP-27 equipment (DCI Corporation) that uses Boyle's law to measure the pore volume at a confining stress (400 psi in this case). The grain volume was measured at ambient conditions using the Accupyc (Micromeritics), again using Boyle's law. The bulk volume was measured submerging the samples in mercury using Archimedes' law.

Permeability was assessed using both a four-point Klinkenberg procedure [6] with nitrogen as medium (Fig. 1, step 2.1e) and an unsteady-state (USS) or pressure decay [24] Klinkenberg test employing helium as the permeant gas (step 2.1f). All measurements were conducted at a constant net confining pressure of 400 psi (27.6 bar) to ensure consistent and representative results.

Table 2. Initial poro-perm data, including a comparison between the Klinkenberg-corrected 4-point measurements [6] and the results from the unsteady-state or pressure decay method [24].

Sample	Grain Density	Helium φ	SS 4-point gas K (N_2)	USS gas K (He)
	g/ml	frac	mD	mD
OBKN1	2.65	0.179	11.5	11.4
OBKN2	2.66	0.180	11.2	10.8
OBKN3	2.66	0.179	10.9	10.2
OBKN4	2.66	0.182	11.9	11.7
C1	3.75	0.569	48.1	46.4
C2	3.75	0.572	48.9	47.5
C3	3.82	0.557	21.1	21.5
C4	3.81	0.551	23.3	23.5

The results obtained from the 4-point steady-state (SS) and unsteady-state (USS) gas permeability measurements show good agreement across all tested samples (see Table 2). We made sure to strictly follow the RP40 guidelines for permissible flow rates, which are based on an estimate of the permeability beforehand and relationships predicting the onset of turbulent flow and compensation for slippage. The values derived from both methods exhibit only minor deviations within experimental uncertainty. This consistency suggests that, under the conditions applied in this study, the SS and USS permeability measurements can be considered equivalent. A statistically rigorous evaluation of the results is presented in Section 2.6

2.2 Absolute oil permeability measurements

The eight cleaned and dried plugs were vacuum saturated with iso-octane to determine absolute oil permeability (see Fig. 3). Iso-octane is a light oil: at 20 °C, the density and viscosity are 0.69 g/ml and 0.573 cP respectively. The saturation process ensured effective pore filling, with measured oil pore volumes ranging between 98% and 102% of the

helium-determined pore volumes, confirming complete saturation.

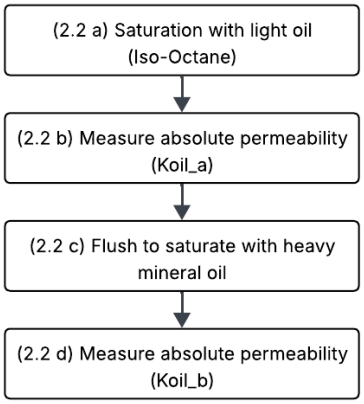

Fig. 3. Flow chart listing the experimental steps for the oil permeability measurements.

Oil permeability measurements were conducted using a Pharmacia P500 precision pump in combination with a hydrostatic core holder. All experiments were carried out under a net confining pressure of 400 psi (27.6 bar) and a backpressure of 72.5 psi (5 bar). Flow was applied in the horizontal direction, and five increasing flow rates, respecting the RP40 recommendations, were used for each sample to assess linearity and Darcy behaviour. Three differential pressure transducers (0–9, 0–36, and 0–100 psi or: 0-0.62, 0-2.5 and 0-6.9 bar) were employed to ensure high resolution and accurate pressure drop measurements across the range of flow conditions.

Following the iso-octane permeability measurements, a second set of absolute oil permeability tests was performed using a high-viscosity oil to investigate the potential influence of oil viscosity on permeability measurements. The high-viscosity oil used in this phase is a blend of two mineral oils (light and heavy oil from Sigma-Aldrich) with a resulting density of 0.834 g/ml and a viscosity of 26.58 cP at 20 °C. Prior to the permeability measurements, the iso-octane was thoroughly displaced by the high-viscosity oil. Complete fluid exchange was confirmed by continuously monitoring the density of the effluent until it matched that of the injected fluid, indicating full saturation of the porous medium.

Absolute permeability with the high-viscosity oil was then measured under identical conditions to those used during the iso-octane experiments, including the same net confining pressure (400 psi, 27.6 bar), backpressure (72.5 psi, 5 bar), flow orientation (horizontal), and range of flow rates, respecting the RP40 recommendations. This ensured comparability of results and facilitated assessment of potential viscosity-dependent flow behaviour.

A statistical analysis (see Section 2.6) of the two sets of absolute oil permeability measurements presented in Table 3—conducted with light oil and with a high-viscosity oil—revealed no significant differences. This indicates, as expected, that oil viscosity does not influence absolute permeability. Furthermore, the absolute oil permeability values obtained with both fluids closely matched the gas permeability values measured previously, again confirming what was expected. A statistical analysis of these results was conducted to obtain unbiased conclusions, see further Section 2.6

Table 3. Oil permeability, comparing low viscosity and high viscosity data with original permeability data.

Sample number	SS gas K (N_2)	USS gas K (He)	K low viscosity oil	K high viscosity oil
	mD	mD	mD	mD
OBKN1	11.5	11.4	11.2	11.7
OBKN2	11.2	10.8	11.1	11.3
OBKN3	10.9	10.2	10.5	10.4
OBKN4	11.9	11.7	11.9	12.2
C1	48.1	46.4	47.3	48.8
C2	48.9	47.5	48.7	49.5
C3	21.1	21.5	21.9	22.4
C4	23.3	23.5	24.3	24.1

2.3 QC steps

Prior to commencing brine permeability measurements, as well as at the end of the whole measurement program, all OBKN plugs were subjected to the same cleaning and drying procedure previously described. This included Soxhlet extraction with an azeotropic mixture of chloroform, methanol, and water, followed by oven drying at 95 °C. This ensured the complete removal of residual oil and salt from the pore space. To verify that the intrinsic properties of the plugs had not changed during the oil/brine testing phase or cleaning process, we re-measured ambient helium porosity and gas permeability under identical conditions to the initial measurements. The results confirmed the consistency of the samples' baseline properties, validating their suitability for the next steps of brine permeability testing. An overview of the data of all consistency checks is presented in Table 10, Section 2.5. No consistency checks have been conducted for the ceramic plugs because these did not show any significant changes (except for C3, see below).

2.4 Brine permeability measurements (high salinity)

The clean and dry plugs were vacuum saturated with a high salinity brine (179,200 ppm total dissolved solids), achieving a saturation level between 98% and 102% of the helium pore volume (see Fig. 4). The ionic composition of the brine is shown in Table 4. Following saturation, the samples were aged under static conditions at ambient temperature for a period of four weeks. Care was taken to exclude oxygen from the system and to shield the brine from direct sunlight in order to prevent any chemical or biological alteration during the aging period.

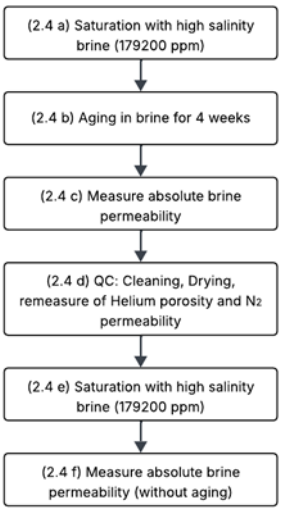

Fig. 4. Flow chart listing the experimental steps for the high salinity brine permeability measurements.

After aging, brine permeability was measured under the same experimental conditions previously used for the oil permeability tests, at five increasing flow rates respecting the RP40 recommendations for liquid flow measurements. The density and viscosity of the brine at 20 °C were 1.12 g/ml and 1.497 cP, respectively.

Table 4. Composition of high salinity brine.

ANIONS [mg/l]		CATIONS [mg/l]	
SO_4^{2-}	15	Na^+	57829
HCO_3^-	77	K^+	370
CO_3^{2-}		Ca^{2+}	8600
Cl^-	110029	Mg^{2+}	1640
		Sr^{2+}	640
		Ba^{2+}	

As shown in Table 5, the results of the brine permeability measurements following the aging process indicated that the OBKN sandstone samples exhibited brine permeabilities consistently lower than their corresponding gas permeabilities, with reductions ranging from 27% to 35%. In contrast, the ceramic samples showed brine permeabilities equivalent to the gas values, with the exception of sample C3. To verify the integrity of this outlier, the sample was cleaned, dried, and re-measured to reassess its base properties. The results revealed a decrease in both porosity and permeability (see Table 6). Because the ceramic samples are 100% Corundum, clay damage can be ruled out suggesting potential damage to, or alteration of the pore structure. We did not investigate this further and sample C3 was excluded from further analysis to maintain data reliability.

Table 5. Permeability with high salinity brine, after four weeks of aging, compared with initial data.

Sample number	SS gas K (N_2)	USS gas K (He)	Kw after aging
	mD	mD	mD
OBKN1	11.5	11.4	8.04
OBKN2	11.2	10.8	7.06
OBKN3	10.9	10.2	7.2
OBKN4	11.9	11.7	8.55
C1	48.1	46.4	46.4
C2	48.9	47.5	47
C3	21.1	21.5	19.1
C4	23.3	23.5	23.3

Table 6. Poro-perm data for ceramic sample C3, cleaned after the high salinity experiment, comparing with initial data.

Sample number	Original φ	Original gas K	New φ	New gas K
	frac	mD	frac	mD
C3	0.557	21.5	0.536	19.9

To assess whether the aging process influenced the brine permeability of the OBKN samples, these were cleaned and dried (Fig. 4, step 2.4d) following the same procedure previously described. Subsequently, these were vacuum saturated with the same high-salinity brine (179,200 ppm) and brine permeability was re-measured at five increasing flow rates without an aging period. This control step (step 2.4f) allowed for a direct comparison, isolating the effect of aging on the measured permeability values.

Table 7. Permeability with high salinity brine, without aging, comparing with data after four weeks of aging and with initial data.

Sample number	SS gas K (N_2)	USS gas K (He)	Kw after aging	Kw without aging
	mD	mD	mD	mD
OBKN1	11.5	11.4	8.04	8.16
OBKN2	11.2	10.8	7.06	7.18
OBKN3	10.9	10.2	7.2	7.03
OBKN4	11.9	11.7	8.55	8.37

The results listed in Table 7 show that the effect of aging in brine is negligible.

2.5 Brine permeability measurements (low salinity)

Following the high salinity brine permeability tests, the brine in all samples (except sample C3) was miscibly displaced (Fig. 5, step 2.5a) with a lower salinity brine (56,422 ppm) to assess the potential impact of salinity on permeability in clean sandstone and artificial ceramic plugs.

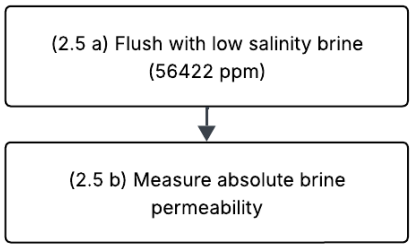

Fig. 5. Flow chart listing the experimental steps for the low salinity brine permeability measurements.

Saturation checks confirmed that brine saturation was between 98% and 102% of the Helium-determined pore volume. The ionic composition of the low salinity brine is detailed in Table 8.

Table 8. Composition of low salinity brine.

ANIONS [mg/l]		CATIONS [mg/l]	
SO_4^{2-}	6	Na^+	14650
HCO_3^-	100	K^+	211
CO_3^{2-}		Ca^{2+}	4800
Cl^-	35026	Mg^{2+}	1027
		Sr^{2+}	602
		Ba^{2+}	

Permeability measurements (step 2.5b) were conducted under the same experimental conditions as the rest of the study—400 psi (27.6 bar) net confining pressure, horizontal sample orientation, and five flow rates. The brine density and viscosity at 20°C are respectively 1.07 g/ml and 1.156 cP. The results show that the permeability values obtained with low salinity brine are comparable to those obtained with high salinity brine. The OBKN sandstone samples again exhibited a consistent reduction in brine permeability relative to gas permeability (Fig. 1, step 2.1e and f), within a range of approximately 30%. In contrast, the ceramic samples maintained permeability values similar to the gas measurements.

A comparative summary of the permeability measurements obtained with gas, high salinity brine, and low salinity brine is presented in Table 9. The results of this experimental program indicate that the observed reduction in brine permeability (~30%) occurs even in clean sandstone samples that do not contain sensitive clay minerals (such as OBKN sandstone). This suggests that in natural reservoir rocks, which often have a higher clay content, the reduction in brine permeability may be potentially even more pronounced. We demonstrated that this reduction is a natural process and cannot be attributed to laboratory procedures or the use of fluids incompatible with the rock matrix.

Indeed, we found consistent data across multiple repetitions, with careful control over saturation levels, physical properties and verification of sample integrity through systematic cleaning and re-measurement protocols.

Table 9. Permeability of low salinity brine comparing with data for high salinity brine and initial data.

Sample number	SS gas K (N_2)	USS gas K (He)	Kw high salinity brine	Kw low salinity brine
	mD	mD	mD	mD
OBKN1	11.5	11.4	8.04	7.91
OBKN2	11.2	10.8	7.06	7.02
OBKN3	10.9	10.2	7.2	7.15
OBKN4	11.9	11.7	8.55	8.56
C1	48.1	46.4	46.4	46.77
C2	48.9	47.5	47	48.33
C4	23.3	23.5	23.3	23.7

In contrast, artificial ceramic samples demonstrated consistent permeability values, independent of the type of saturating fluid—whether polar or non-polar—highlighting the absence of fluid-solid interactions in such media.

Finally, Table 10 gives an overview of the QC data, and comparing these to the initial poro-perm data for OBKN plugs. Apart from C3, the ceramic plugs were not subjected to separate QC, because no important changes in base poro-perms were seen during the measurement sequence. Reproducibility appears to be excellent.

The observed reduction in brine permeability in outcrop samples is most likely associated with physical and chemical interactions between the grains and rock surface and ions present in the brine. These interactions, potentially driven by ionic forces such as electrical double-layer effects or specific ion adsorption, appear to influence the flow behaviour in the porous media. Such effects are expected to be even more pronounced in formations containing reactive or clay-rich components and should therefore be carefully considered when choosing the reference permeability in a relative permeability experiment or simulation.

Table 10. Columns 2 and 3 refer to original poro-perm data. The next two columns refer to the re-runs after the absolute oil permeability and the last two columns show porosity and permeability at the end of the experimental program.

Sample	He φ	SS gas K (N_2)	He φ	SS gas K (N_2)	He φ	SS gas K (N_2)
	frac	mD	frac	mD	frac	mD
OBKN1	0.179	11.5	0.175	11.6	0.177	11.4
OBKN2	0.180	11.2	0.178	11.4	0.177	11.6
OBKN3	0.179	10.9	0.176	10.5	0.178	10.1
OBKN4	0.182	11.9	0.178	11.6	0.183	12.1

2.6 Statistical analysis

Applied statistics is a mathematical discipline that supports researchers making the correct analysis and interpretation of their data and thus overrule subjective statements that may not be valid. Klinkenberg [6] showed that there was no difference between the liquid permeability and the (slip corrected) gas permeability for "clean" rocks. The primary claim in our study is that the gas permeability is observed to be larger than the

absolute brine permeability even for clean rocks, and this may cause an unexpected problem in normalising relative permeabilities in CCS drainage experiments. To investigate such an issue it is normal practice in statistical analysis to formulate a "null hypothesis H_0" of there being no difference between the observations. The objective will then be to formally accept or reject this statement. Our H_0 therefore is set-up as "There is no difference between the gas permeability and the liquid permeabilities measured for OBKN sandstone and synthetic porous ceramic samples".

First we have to make some observations and select the right tools for the statistical analysis. For porous media we will assume that porosity has a normal distribution and that permeability has a log-normal distribution [25, 26]. We notice that in our study as well as many other SCAL studies, the number of plugs is less than 10, i.e. we have to use "small sample statistics" in our analysis. We have selected the Students t-test to judge differences between means of the measured permeabilities, and selected the F-test for analysis of variance. An introduction to applied statistics relevant to our study can be found from Numerical Recipes [27] that is accessible through the internet.

The work flow is then to determine first the mean $\bar{X}_i$ and standard deviation s_i of each data set, see Table 11. Note that the calculation of the mean $\bar{X}$ for porosity is straightforward, but for permeability it is calculated as the geometric mean due to the log-normal distribution.

Subsequently, the F-test on the variances is evaluated to establish the correct formula to calculate the t-test value t_{calc} for two different means:

$$t_{calc} = \frac{(\overline{X_1} - \overline{X_2})\sqrt{\frac{N_1 N_2}{N_1 + N_2}}}{\sqrt{\frac{(N_1-1){s_1}^2 + (N_2-1){s_2}^2}{N_1 + N_2 - 2}}} \qquad (1)$$

Finally, t_{calc} is then compared to t_{table}, a value found in the table of the t-probability distribution [28] at degrees of freedom $df = N_1 + N_2 - 2$ where N_1 and N_2 are the number of measurements in the two sample sets being compared. The tables are available at certain "significance levels". For our analyses we have selected a significance level of 5% in line with common practice. The formal meaning of that is that if an H_0 hypothesis is rejected at the 5% level it is expected that the chances are only 5% at maximum that this rejection would be wrong.

If t_{calc} is seen to be less than t_{table}, we have an objective assessment that the statement H_0 is true, meaning in our case that the difference between the two means under consideration is non-significant at the chosen level.

We have conducted several analyses of the permeability measurements as follows. In Table 12 we show the comparison between the steady-state gas (N_2) permeability, used as a common base case, with the gas permeability measured using the unsteady-state method and with the liquid permeabilities measured with light oil, with high viscous oil, with high salinity brine and with the low salinity brine.

Table 11. Results for mean values for the measurements on the OBKN and ceramic plugs. Sample C3 was discarded after it showed permanent damage (see Section 2.4 and Table 6). The 95% Confidence Interval CI_{95} is given as $\bar{X} \pm c$ with $c = t_{95} \times [\, s_i / \sqrt{N}]$, where t_{95} is the 95% probability data extracted from a table of the t-probability distribution [28] at degrees of freedom $df = N-1$ where N is the number of measurements in a sample set. CI_{95} denotes that 95% of sample means are expected to fall within the listed interval and is an indication of the quality of the lab data. In general, a large N will generate a narrow CI, while a small N will cause a large CI. A log-normal distribution is not symmetrical, i.e. + CI and - CI is not similar; therefore CI is given with its upper and lower bound in the tables below. For the meaning of "pooled data" we refer to [27].

OBKN Permeability (mD)			
Subject test: ↓	$\bar{X}$	*CI 95%*	*N*
SS K gas (N2)	11.3	11.7-10.9	8
USS K gas (He)	11	12.1-10.0	4
Light oil	11.2	12.1-10.3	4
Viscous oil	11.4	12.7-10.2	4
High salinity brine	7.7	8.2-7.2	8
Low salinity brine	7.6	8.8-6.6	4
C1+C2 Permeability (mD)			
Subject test: ↓	$\bar{X}$	*CI 95%*	*N*
SS K gas (N2)	48.5	53.9-43.7	2
USS K gas (He)	47	54.0-40.9	2
Light oil	48	57.8-39.9	2
Viscous oil	49.1	53.9-44.8	2
High salinity brine	46.7	50.3-43.4	2
Low salinity brine	47.5	58.6-38.6	2
C4 permeability (mD)			
Subject test: ↓	$\bar{X}$	*CI 95%*	s_i
all fluids, pooled data	23.7	24.1 - 23.3	0.4

We have $t_{calc} < t_{table}$ for each of the non-reactive fluids (gasses and oils) which gives us an objective view on that there are no significant differences (non-S) between the gas permeability and the permeability measured for these fluids. Observe also that the USS results are not significantly different from the base SS results. On the other hand, the two different brines tested very significant at the 5% level against the N_2 SS gas permeability. A lookup in the t-tables showed they are also different from the SS gas even at the 0.1% level, meaning that there is a 99.9% chance that the brine permeabilities objectively are truly different from the base gas permeability.

Our set of different liquids makes it possible also to check for differences due to liquid type.
The H_0 hypothesis: "There is no significant difference between the test liquids" is tested in the table 13.

Table 12. t-test conducted at 5% significance level, OBKN plugs and ceramic plugs C1 and C2.

t-test: SS K gas (N2) vs other fluid on OBKN plugs			
Subject test: ↓	t_{calc}	t_{table}	Result
USS K gas (He)	0.85	2.2	non-S
Light oil	0.47	2.2	non-S
Viscous oil	0.21	2.2	non-S
High salinity brine	12	2.1	S
Low salinity brine	11	2.2	S
t-test: SS K gas (N2) vs other fluid on C1+C2			
Subject test: ↓	t_{calc}	t_{table}	Result
USS K gas (He)	2.4	4.3	non-S
Light oil	0.6	4.3	non-S
Viscous oil	1.2	4.3	non-S
High salinity brine	3.7	4.3	non-S
Low salinity brine	1.1	4.3	non-S

We see that for each pair of liquids, the differences in permeability are non-significant in the ceramic samples C1 and C2. For the OBKN plugs that is true comparing one oil with the other, or one brine with the other. Only comparing brine permeability with the oil permeability showed a significant difference at the 5% significance level for OBKN. As before, a further lookup in the t-tables showed that these are also different even at the 0.1% level.

Table 13. Test for permeability differences between 2 liquids, at 5% significance level, split out over OBKN and the ceramic plugs. Observe that the only significant result occurs for the light oil vs high salinity brine on OBKN, and that it is extremely significant (S). There is no significant difference between the two brines, and no significant differences at all for the ceramic samples.

t-test : OBKN liquids			
Subject test: ↓	t_{calc}	t_{table}	Result
Light oil vs. Viscous oil	0.4	2.4	non-S
Light oil vs. high salinity brine	8.1	2.2	S
High salinity vs. low salinity brine	0.1	2.2	non-S
t-test : C1+C2 liquids			
Subject test: ↓	t_{calc}	t_{table}	Result
Light oil vs. Viscous oil	1.4	4.3	non-S
Light oil vs. high salinity brine	1.7	4.3	non-S
High salinity vs. low salinity brine	1	4.3	non-S

Finally, due to C3 is missing, the C4 is a stand-alone with statistics (Table 11) given as the mean of the 6 different fluid measurements from Tables 3 and 5. No single measurement deviated more than 1 standard deviation from the mean, i.e. there was no indication of reduced brine permeability for this low porosity ceramic sample.

3 Impact of relative permeability being larger than unity

Now that we have established that the brine permeability being smaller than the gas permeability is not a laboratory artefact, we will address the implications of that in the laboratory as well as for reservoir engineering simulations.

3.1 Implications for laboratory protocols

We recall that relative permeability k_r is defined through an empirical extension of the single-phase Darcy equation as follows (see e.g. Dake [4]):

$$q_i = \frac{k_{ri}}{\mu_i} K \frac{\Delta P}{L} \qquad (2)$$

in which q is the flow rate, i identifies the phase (water/oil/gas), μ_i is the viscosity of the fluid i, K is the absolute permeability, and ΔP is the pressure drop across the plug length L. In analysing laboratory experiments, k_{ri} always appears in a product together with the absolute permeability K, irrespective of which analysis is used. We list here: JBN [29] analysis for unsteady-state experiments with liquids at constant injection rate or for unsteady-state experiments with gas at constant ΔP; or the use of Eq. 2 directly for steady-state experiments; or the Hagoort [30] analysis of single-speed centrifuge experiments.

As also mentioned in Section 1, in the industry various approaches are used to normalise relative permeabilities, e.g. normalise to K_{brine} at $S_w = 1$, to K_{oil} at S_{wc}[2], or even have $k_r = 1$ defined for each phase separately. A SCAL report will list what normalisation was done. Since k_{ri} always "lives" in a product together with the absolute permeability, the analysis method itself will be insensitive to the choice of K_{abs} while clearly the k_{ri} data are scaled accordingly and therefore change with the choice of K_{abs}. This is further demonstrated below where we address the impact of k_{ri} being larger than unity in flow simulations. Meanwhile, we conclude that laboratory protocols and analysis methods are not affected by k_{ri} being larger than unity.

3.2 Implications on simulations

Relative permeability being larger than unity does have an impact on simulation work, simply because commercial flow simulators just do not accept k_r data above unity. Such data are declared to be invalid input. To verify and prove that analysis methods indeed are insensitive to k_r being above unity, we have modified SCORES (our flow simulator that we make available at no cost [31, 32]) and removed temporarily the restriction on k_r that also we originally had built- in. We ran flow simulations for an unsteady-state drainage experiment with oil displacing brine, with bump flood, in two

[2] We use the convention that the connate water saturation S_{wc} indicates the immobile water saturation rather than a (possibly mobile) initial water saturation.

different input configurations: case a) using a k_{ro} normalised to K_{brine} with an end-point of 1.63 at S_{wc}, while K_{abs} = 100 mD; b) using the k_{ro} data now re-normalised to $K_{abs} = K_{gas}$ = 166.7 mD, so k_{ro} values are all below unity. Note that to have consistent relative permeability data, the k_{rw} data had to be normalised in sync with the k_{ro} data. Input data for the SCORES simulations are listed in Tables 14, 15 and 16.

Table 14. Rock and fluid data used in the simulations

L (cm)	4.57	D (cm)	3.75
φ (-)	0.184	K (mD)	166.7 or 100
ρ_w (g/ml)	1.015	ρ_o (g/ml)	0.76
μ_w (cP)	0.976	μ_o (cP)	2.94

Fig. 6 shows that the production profiles generated with these two different normalisations are identical. Moreover, the saturation profiles (discussed in Section 4, Fig. 7) are also identical. So, indeed the laboratory protocols do not need to be modified if one would allow relative permeability to become larger than unity. Note that the equality of the production data was the expected result analysing the flow equations, discussed in Section 3.1.

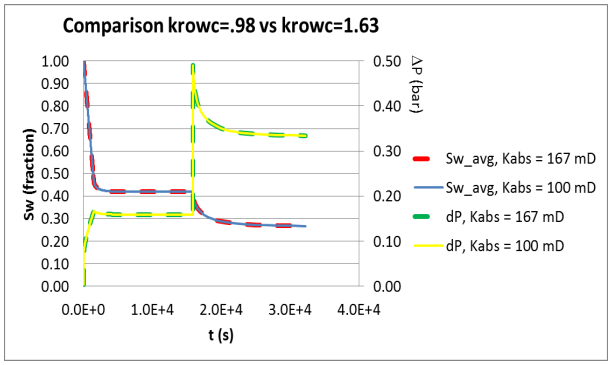

Fig. 6. Simulated average water saturation and pressure drop across the sample for a drainage unsteady-state experiment with q_{inj} = 0.2 ml/min, bump flood with q_{inj} = 1 ml/min at t = 265 min comparing with the results obtained with relative permeabilities scaled with respect to K_{abs} = 166.7 or 100 mD respectively. Note k_{rowc} = 0.98 for K_{abs} = 166.7 mD and k_{rowc} = 1.63 with K_{abs} = 100 mD (see Table 15). The curves overlay perfectly.

There remains one issue to be dealt with when re-normalising relative permeability to a different absolute permeability. In the event that one uses a capillary pressure curve in the simulations that is defined through a scaling to a dimensionless Leverett-J curve, the resulting capillary pressure curve would change due to the different value for the absolute permeability being used, see Eq. 3.

$$P_c(S_w) = \sigma cos\theta \sqrt{\frac{\varphi}{K}} J(S_w) \qquad (3)$$

in which P_c is the capillary pressure function of the water saturation S_w, σ is the interfacial tension (IFT) between water and the other phase, θ is the contact angle between the two phases, and φ is the porosity. Typically, this issue comes about in automatic history matching, e.g. with AutoSCORES [23, 33], matching two or more different experiments on different plugs (e.g. a flow experiment and a multi-speed centrifuge experiment) with one common data set for relative permeabilities and capillary pressure defined through a Leverett-J function. The issue is easily resolved by adjusting IFT.

Table 15. Relative permeability data scaled to K_{abs} = 100 mD and to K_{abs} = 167 mD

	Kabs = 100 mD		Kabs = 167 mD	
Sw	krw	kro	krw	kro
0.05	0	1.633333	0	0.98
0.144	5.25E-05	1.228937	3.15E-05	0.737362
0.238	0.000966	0.894165	0.00058	0.536499
0.332	0.005306	0.623505	0.003183	0.374103
0.426	0.017761	0.411228	0.010657	0.246737
0.52	0.045341	0.251358	0.027205	0.150815
0.614	0.097511	0.137606	0.058507	0.082564
0.708	0.186308	0.063285	0.111785	0.037971
0.802	0.326435	0.021177	0.195861	0.012706
0.896	0.53535	0.003259	0.32121	0.001955
0.99	0.833333	0	0.5	0

Table 16 Capillary pressure table

Sw	Pc (bar)
0.05	9.830
0.12	6.389
0.14	0.491
0.26	0.216
0.44	0.098
0.56	0.075
0.69	0.065
0.76	0.062
0.86	0.060
0.97	0.058
0.99	0.000

In field simulations, Leverett-J scaling does occur probably more frequently, to define capillary pressure functions locally dependent on rock types with different porosity and absolute permeability. An approach with modified IFT will resolve the issue, similar to as mentioned above.

In summary: relative permeability values above unity generally cannot be handled by simulators, but that is not a problem. Identical results can be generated by re-normalising the relative permeabilities with the absolute gas permeability. A correction may be needed only in the case of Leverett-J scaled capillary pressure functions.

4 Impact on CCS screening

SCAL data are part of the basic data feeding reservoir engineering models. Therefore SCAL measurement programs need to be tailored to a field development plan. We will now discuss some implications for CCS engineering that are different from engineering conventional water drive projects for oil reservoirs.

CCS is about injection of (usually super-critical) CO_2 into aquifers, oil fields or gas fields. Therefore, CCS into aquifers or oil fields require drainage experiments, contrary to SCAL for water drives that require imbibition experiments. Interestingly, the initial steps of a SCAL program for CCS are the same as for water drives: the measurement of porosity and gas permeability, followed with saturating the core plug with a representative brine, and measuring K_{brine}. SCAL for water drive projects then requires flooding the core plug with oil, displacing the brine to a representative initial water saturation S_{wi}. Subsequent experiments with water displacing oil to measure imbibition relative permeabilities may then use K_{brine} as reference permeability.

SCAL measurements for CCS do use injection of a non-wetting phase viz. CO_2 [34] after measuring K_{brine}, but at that point already the production data are used to derive the drainage relative permeabilities. It is generally believed [35, 36] that sandstones as well as carbonates are mainly water-wet if these have not been in contact with oil. Drainage capillary pressure curves of water-wet rock are characterised by dimensionless Leverett-J functions with a plateau value of around 0.4 [3] at mid-range saturations. So, drainage capillary pressure curves are very different from imbibition capillary pressure curves seen in oil reservoirs: these show plateau values close to zero over an extended saturation range [37].

This means that drainage experiments with CO_2 for sequestration in aquifers may suffer from significant end-effects in the core plug, such as shown in Fig. 7.

The profiles in Fig. 7 were generated with the drainage simulations discussed in Section 3. In imbibition experiments with water displacing oil, the result of an end-effect is that the oil saturation remaining after water flooding a core plug is 0.1 to 0.15 saturation units higher than the true residual oil saturation [38]. In drainage experiments with CO_2 displacing brine, one sees a mirror image of that: the remaining water saturation may be much larger than the true connate water saturation. With the understanding that capillary pressure curves show an asymptote going to negative infinity at S_{or} for imbibition and to positive infinity at S_{wc} for drainage, it is clear that it is impossible to fully overcome the capillary pressure. We cannot emphasize strongly enough that this remains true even at high rates: infinity is always just too far away. The observation in the lab that the displaced phase stopped moving therefore cannot be just attributed to a relative permeability of that phase being zero; it may well be that capillary pressure has taken over in blocking the flow.

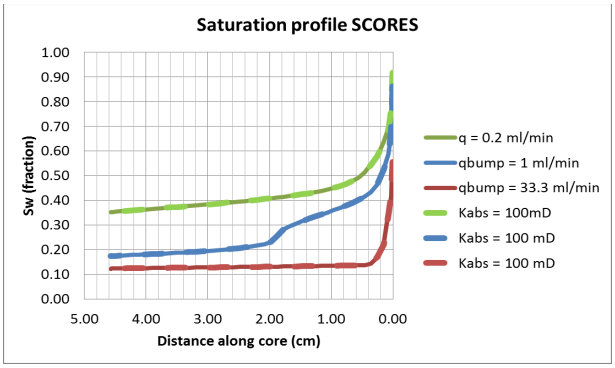

Fig. 7. Comparison of simulated water saturation profile at the end of the bump flood (blue) with the profile just before the bump (green) of the drainage experiment discussed in Section 3. The solid lines were simulated with relative permeabilities scaled to K_{abs} = 167 mD; the dashed lines with relative permeabilities scaled to K_{abs} = 100 mD. As in Fig. 6, the curves overlay perfectly. The shape is typical for a strong water-end-effect. Injection is at the left. Note that S_{wc} (see Tables 15 and 16) was input as 0.05, but not reached anywhere in the core plug, not even at the end of the bump flood of 1 ml/min, nor when the bump was increased to 33.3 ml/min (red curve).

Only by history matching with e.g. AutoSCORES of a flow experiment in combination with a multi-speed centrifuge experiment (designed to measure capillary pressure), one can try to unravel this ambiguity. In addition, the plateau value of a drainage curve, seen when water is displaced, usually is much higher than for mixed-wet imbibition capillary pressure curves where water is displacing oil. Therefore, the difference between the remaining water saturation and S_{wc} during CO_2 injection is also much higher than between remaining oil and S_{or} in water floods.

We now need to consider the situation around the injection well in CCS into an aquifer, to understand how to design SCAL flow experiments for collecting data representative of the field. Close to the injector, one expects that the remaining water saturation will be negligible, due to several processes combined: evaporation and/or dissolution of water into CO_2 and desaturation due to high-capillary-number flow. This will bring about an effective permeability to CO_2 close to, or equal to the gas permeability. Therefore, one needs to design SCAL flow experiments to cover such saturations, despite the capillary end-effect. Without such design, remaining water saturations are expected to be much higher than the true S_{wc}, and the measured effective gas permeability is then likely to be much lower than the absolute gas permeability. This may well explain that it is relatively rare for effective permeabilities to become larger than the brine permeability. Still such observations have been published [39, 40].

The understanding that the CO_2 effective permeability should approach the gas permeability has an important effect on the screening of reservoirs for CCS. Well injectivity is proportional to permeability [e.g. 41] and CCS project economics depend strongly on injectivity [42, 43, 44]. High injectivity enhances project economics because it impacts on the well count for a

projected total injected volume over a given time-span. Choosing for permeability the Klinkenberg-corrected gas permeability instead of the brine permeability may have a major impact, certainly if the brine permeability is half or even only 10% of the gas permeability.

5 Conclusions and Recommendations

- A rigorous statistical analysis has been conducted on absolute permeability measurements, precluding subjective conclusions on observed differences in permeability when flooding with brine compared to absolute gas and absolute oil permeability in Obernkirchener (OBKN) sandstone plugs.
- No such statistically significant differences were found during the measurement of absolute permeability on ceramic plugs.
- Aging the OBKN plugs in brine did not impact the result of the permeability measurement.
- Brine permeability at $S_w = 1$ being lower than gas absolute permeability in OBKN plugs is not a laboratory artefact and is likely the impact of electrical forces on pressure drop.
- Conversely, the effective permeability of oil or gas being larger than the absolute brine permeability does not require anymore an explanation through a "lubrication effect".
- Relative permeabilities larger than unity are a viable measurement result.
- Relative permeabilities normalised to the brine permeability can be renormalised to the gas permeability, while generating identical results in production and saturation profiles.
- For CCS, we recommend using the Klinkenberg corrected gas permeability as absolute permeability to normalise relative permeabilities. Resulting relative permeabilities will be less than unity and therefore will not be rejected anymore by commercial simulators.
- Because brine permeabilities that conventionally are used to normalise relative permeabilities are often significantly lower than the gas permeability, the proposed re-normalisation will have significant impact on screening for CCS. Projected injectivity will proportionally be enhanced, reducing projected development costs.
- Only in the event that Leverett-J functions for capillary pressure are used in the numerical modelling, a correction need to be applied when re-normalising relative permeabilities. This is easily done by adjusting the interfacial tension in the simulation models.

Nomenclature

CI_n	Confidence Interval
df	Degrees of freedom
D	Diameter [m]
K	Permeability [m^2]
L	Length [m]
N	Number of measurements
Non-S	Insignificant at the specified test level
ΔP	Pressure drop across sample [Pa]
P_c	Capillary pressure [Pa]
q	flow rate [m^3/s]
s_i	Standard deviation
s_i^2	Variance
S	Significant at the specified test level
t_n	t-statistic
$\bar{X}$	Sample mean (geometric)

Greek

θ	contact angle [degrees]
φ	Porosity [-]
μ	Viscosity [Pa.s]
ρ	Density [kg/m^3]
σ	Interfacial tension [N/m]

Subscripts

abs	absolute
calc	calculated
i	phase: oil/water/gas
i	Sample numbering
inj	injection
n	probability for *t* or *CI* given as a %
o	oil
r	relative
table	quantity extracted from a table
w	water
wc	connate water

The CT-scans of the ceramic plugs and OBKN material were made available courtesy of Prof. Hemmo Abels, TUDelft, and conducted expertly by Mrs. Ellen Meijvogel - de Koning, TUDelft.

References

1. H. Darcy, "Les Fontaines publiques de la ville de Dijon: exposition et application des principes à suivre et des formules à employer dans les questions de distribution d'eau", Dalmont, Paris (1856).
2. A.E. Scheidegger, "The physics of flow through porous media", Macmillan Co, New York (1957).
3. R.E. Collins, "Flow of fluids through porous materials", Litton Educational Pub Inc, (1961).
4. L.P. Dake, "Fundamentals of reservoir engineering", Elsevier, Amsterdam (1978).
5. H.R. Warner, Jr., "The reservoir engineering aspects of waterflooding, second edition", SPE Monograph series, Vol. 3 (2015).
6. L.J. Klinkenberg, "The permeability of porous media to liquids and gases", API Drilling and Production Practice 200-213 (1941).
7. S.S. Chhatre, H. Sahoo, S. Leonardi, K. Vidal, J. Rainey, E.M. Braun, P. Patel, "A blind study of four digital rock physics vendor laboratories on porosity, absolute permeability, and primary drainage capillary pressure data on tight outcrops", SCA2017-004 (2017).
8. T. Orlander, H. Milsch, I.L. Fabricius, "Comparison of gas, Klinkenberg, and liquid permeability of sandstone: flow regime and pore size", AAPG Bull. 107(7), 1383-1403 (2021), DOI: 10.1306/12222019138
9. A.M. Saidi, "Effect of clays on the permeability of reservoir sandstone to various brines", Thesis, Colorado School of Mines, Golden, CO, USA (1958)
10. W. Tanikawa, T. Shimamoto, "Klinkenberg effect for gas permeability and its comparison to water

permeability for porous sedimentary rocks", Hydrol. Earth Syst. Sci, Discuss. **3**, 1315-1338 (2006)

11. I. Ahmad, M. Ahmad, I. Ali, "Klinkenberg-corrected and water permeability correlation for a Serawak carbonate field", Fluids **6**, 339 (2021).
12. I.A.M. Zaidi, M. Ahamad, M.G. Baboli, "Comparison between Klinkenberg-corrected and water permeability: a review", ARPN J. Eng, Appl, Sci, Vol 14, No 19, 3437-3443 (2019).
13. A. Cable, M. Burke, "Investigation of permeability anomalies", SCA2011-11 (2011).
14. C.A. McPhee, K.G. Arthur, "Relative permeability measurements: an inter-laboratory comparison", SPE 28826 (1994).
15. M. Mikkelsen, A. Scheie, "abnormal permeability behaviour of a North Sea sandstone reservoir", SPE 22600 (1991).
16. A. Cable, D. Mogford, M. Wannell, "Mobilisation of trapped gas from below the gas-water contact", SCA2004-29 (2004).
17. H. Bertin, W. AlHanai, A. Ahmadi, M. Quintard, "Two-Phase flow in heterogeneous nodular porous media", SCA1992-23EURO (1992).
18. S. Berg, A.W. Cense, J.P. Hofman, R.M.M. Smits, "Flow in porous media with slip boundary condition", SCA2007-13 (2007).
19. F. Pairoys, D. Simons, K. Bohm, M. Alexander, V. Odu, R. DeLeon, J. Ramos, "Effect of the presence of interstitial brine on gas-oil capillary pressure", SCA2015-015 (2015).
20. S.K. Masalmeh, "Experimental measurements of capillary pressure and relative permeability hysteresis", SCA2001-23 (2001).
21. "Recommended practices for Core analysis, Report RP 40", 2nd edition, Exploration and Production Dept., American Petroleum Institute (1998).
22. M. Halisch, F. Pairoys, C. Caubit, Th. Grelle, "Assessing the impact of dopants on electrokinetic rock properties as potential indicators for dopant induced wettability changes", SCA2024-1031(2024)
23. J.G. Maas, N. Springer, A. Hebing, "Defining a sample heterogeneity cut-off value to obtain representative Special Core Analysis (SCAL) measurements", SCA2019-024 (2019).
24. S.C. Jones, "A rapid accurate unsteady-state Klinkenberg permeameter", Soc. Pet. Eng. J., 12(5), 383–397 (1972).
25. F. Dullien, "Porous Media: fluid transport and pore structure", Academic Press, New York (1991), 139-176.
26. J.H. Doveton, "Principles of Mathematical Petrophysics", Ch. 3. Oxford Academic, 2014. https://doi.org/10.1093/oso/9780199978045.003.0008
27. W.H. Press, B.P. Flannery, S.A. Teukolsky, W.T. Vetterling, Numerical Recipes in C++, The Art of Scientific Computing, 2nd Edition, Cambridge University Press, Cambridge (2002). See also http://www.numerical.recipes
28. R.A. Fisher, F. Yates, "Statistical tables for biological, agricultural and medical research", London, Oliver & Boyd (1963).
29. E.F. Johnson, D.P. Bossler, V.O. Naumann, "Calculation of relative permeability from displacement experiments", AIME **216**, 370–372 (1958).
30. J. Hagoort, "Oil recovery by gravity drainage", SPE 7424 (1980).
31. J.G. Maas, B. Flemisch, A. Hebing, "Open source simulator DuMu^x available for SCAL data interpretation", SCA2011-08 (2011).
32. R. Lenormand, K. Lorentzen, J.G. Maas, D. Ruth, "Comparison of four numerical simulators for SCAL experiments", SCA2016-006 (2016).
33. J.G. Maas, N. Springer, A. Hebing, J. Snippe, S. Berg, "Viscous fingering in CCS - A general criterion for viscous fingering in porous media", IJGGC, Vol 132, Feb 2024, 104074, https://doi.org/10.1016/j.ijggc.2024.104074 (2024).
34. W.-J. Plug, S. Mazumber, J. Bruining, "Capillary pressure and wettability behaviour of CO_2 sequestration in coal at elevated pressures", SPE108161(2008).
35. H. Sharma, K.K. Mohanty, "An experimental and modeling study to investigate brine-rock interactions during low-salinity water flooding in carbonates", J. Petr. Sc. Eng. **165**, p 1021-1039 (2018).
36. J.S. Buckley, "Mechanisms and consequences of wettability alteration by crude oils", Thesis, Heriot-Watt University, UK (1996).
37. J. Reed, J.G. Maas, "Review of the intercept method for relative permeability correction using a variety of case study data", SCA2018-030 (2018).
38. J.E. Nordtvedt, H. Urkedal, E. Ebeltoft, K. Kolltveit, E.B. Petersen, A. Sylte, R. Valestrand, "The significance of violated assumptions on core analysis results", SCA-9931 (1999).
39. Y.C. Araujo de Itriago, S. Devier, P. Singletary, H. Watkins, "Accurate measurement of relative permeability as crucial step for carbon capture, utilization and storage: case study", SPE-220983-MS (2024).
40. S. Berg, A.W. Cense, J.P. Hofman, R.M.M. Smits, "Flow in porous media with slip boundary condition", SCA2007-13 (2007).
41. W.C. Lyons, G.J. Plisga, M.D. Lorenz, "Standard handbook of petroleum and natural gas engineering", 3rd Ed., Elsevier (2016).
42. P.M. Jarrell, C.E. Fox, M.H. Stein, S.L. Webb, "Practical aspects of CO_2 flooding", SPE Monograph series, Vol. 22 (2002)
43. IEAGHG, "Injection strategies for CO_2 storage sites", report 2010/04, June 2010 (2010).
44. G. Sun, Z. Sun, A. Fager, B. Crouse, "Pore-scale analysis of CO_2-brine displacement in Berea sandstone and its, implications to CO_2 injectivity", SCA2022-37 (2022).